

The effect of cooling on the global stability of self-gravitating protoplanetary discs

W.K.M. Rice¹, P.J. Armitage^{2,3}, M.R. Bate⁴ and I.A. Bonnell¹

¹*School of Physics and Astronomy, University of St Andrews, North Haugh, St Andrews KY16 9SS*

²*JILA, Campus Box 440, University of Colorado, Boulder CO 80309-0440, USA*

³*Department of Astrophysical and Planetary Sciences, University of Colorado, Boulder CO 80309-0391, USA*

⁴*School of Physics, University of Exeter, Stocker Road, Exeter EX4 4QL*

1 November 2018

ABSTRACT

Using a local model Gammie (2001) has shown that accretion discs with cooling times $t_{\text{cool}} \leq 3\Omega^{-1}$ fragment into gravitationally bound objects, while those with cooling times $t_{\text{cool}} > 3\Omega^{-1}$ evolve into a quasi-steady state. We use three-dimensional smoothed particle hydrodynamic simulations of protoplanetary accretion discs to test if the local results hold globally. We find that for disc masses appropriate for T Tauri discs, the fragmentation boundary still occurs at a cooling time close to $t_{\text{cool}} = 3\Omega^{-1}$. For more massive discs, which are likely to be present at an earlier stage of the star formation process, fragmentation occurs for longer cooling times, but still within a factor of two of that predicted using a local model. These results have implications not only for planet formation in protoplanetary discs and star formation in AGN discs, but also for the redistribution of angular momentum which could be driven by the presence of relatively massive objects within the accretion disc.

Key words: accretion, accretion discs — planetary systems: protoplanetary discs — planetary systems: formation — stars: formation — stars: pre-main sequence — galaxies: active

1 INTRODUCTION

The formation of substellar companions within protoplanetary discs has received a great deal of attention since the first observation of an extra-solar planet (Mayor & Queloz 1995). To date many additional extrasolar planets have been observed (see Marcy & Butler 2000 for a review), further fueling the interest in the formation of planets and the evolution of protoplanetary discs. The most widely studied planet formation mechanism is core accretion (see Lissauer 1993) in which planetismals grow by direct collisions to form a core which, when sufficiently massive ($m \sim 10m_{\text{earth}}$) then accretes an envelope of gas from the disc.

An alternative mechanism for giant planet formation is via the gravitational instability (Kuiper 1951; Boss 1998, 2000). This differs from core accretion in that a rocky core is not initially required and the process is extremely rapid. A Keplerian accretion disc with sound speed c_s , surface density Σ , and epicyclic frequency κ will become gravitationally unstable if the Toomre (1964) Q parameter

$$Q = \frac{c_s \kappa}{\pi G \Sigma} \quad (1)$$

is of order unity. A gravitationally unstable disc can either fragment into one or more gravitationally bound objects,

or it can evolve into a quasi-stable state in which gravitational instabilities lead to the outward transport of angular momentum. The exact outcome depends on the rate at which the disc heats up (through the dissipation of turbulence and gravitational instabilities) and the rate at which the disc cools. It has been suggested (Goldreich & Lynden-Bell 1965) that a feedback loop may exist where when Q is large cooling dominates and the disc is cooled towards instability. When Q becomes sufficiently small, heating through viscous dissipation dominates and the disc is returned to a state of marginal stability. In this way Q is maintained at a value of ~ 1 .

Gammie (2001) has, however, shown using a local model that a quasi-stable state can only be maintained if the cooling time $t_{\text{cool}} > 3\Omega^{-1}$ where Ω is the local angular frequency. For shorter cooling times, the disc fragments. This finding is consistent with Pickett et al. (1998, 2000) that ‘almost isothermal’ conditions are necessary for fragmentation, and defines a robust lower limit to the critical cooling time below which fragmentation occurs. It has been suggested, however, that self-gravitating discs strictly require a global treatment (Balbus & Papaloizou 1999), and while global effects are highly unlikely to stabilize a locally unstable disc, they could well allow fragmentation within discs that would locally be

stable. In this paper we use a global model to test whether a gaseous accretion disc still fragments for $t_{cool} \leq 3\Omega^{-1}$ and attains a quasi-stable state for $t_{cool} > 3\Omega^{-1}$. Although our choice of parameters is more appropriate for protoplanetary accretion discs, the results may also be applicable for star formation in AGN discs, which are expected to become gravitationally unstable at large radii (Shlosman & Begelman 1989; Goodman 2002), and for star formation in the gaseous regions of spiral galaxies (Kim & Ostriker 2002).

2 NUMERICAL SIMULATIONS

2.1 Smooth particle hydrodynamics code

The three-dimensional simulations presented here were performed using smoothed particle hydrodynamics (SPH), a Lagrangian hydrodynamics code (e.g., Benz 1990; Monaghan 1992). In this simulation the central star is modelled as a point mass onto which gas particles can accrete if they approach to within the sink radius, while the gaseous disc is simulated using 250,000 SPH particles. Both point masses and gas use a tree to determine neighbours and to calculate gravitational forces (Benz et al. 1990), and the point mass representing the central star is free to move under the gravitational influence of the disc gas. Although the code can in principle continue running if the disc starts to fragment and high density regions form, it quickly becomes too slow to realistically continue in this manner. To continue simulating a fragmenting disc, point masses are created (Bate et al. 1995) if the high density regions are gravitationally bound (gravitational potential energy at least twice the thermal energy). As with the point mass representing the central star, point masses within the disc may continue to accrete gas particles if they fall within the sink radius. An additional saving in computational time is also made by using individual, particle time-steps (Bate et al. 1995; Navarro & White 1993). The time-steps for each particle are limited by the Courant condition and a force condition (Monaghan 1992).

2.2 Initial conditions

We consider a system comprising a central star, modelled as a point mass with mass M_* , surrounded by a gaseous circumstellar disc with mass M_{disc} . Most of the simulations presented here considered a disc mass of $M_{\text{disc}} = 0.1M_*$, but a few were performed using $M_{\text{disc}} = 0.25M_*$. The disc temperature is taken to have an initial radial profile of $T \propto r^{-0.5}$ (e.g., Yorke & Bodenheimer 1999) and the Toomre Q parameter is assumed to be initially constant with a value of 2. A stable accretion disc where self-gravity leads to the steady outward transportation of angular momentum should have a near constant Q throughout. A constant Q together with equation (1) then gives a surface density profile of $\Sigma \propto r^{-7/4}$, and hydrostatic equilibrium in the vertical direction gives a central density profile of $\rho \propto r^{-3}$.

The disc is modelled using 250,000 SPH particles, which are initially randomly distributed in such a way as to give the specified density profile between inner and outer radii of r_{in} and r_{out} respectively.

The calculations performed here are essentially scale free. In code units, we take $M_* = 1$, $r_{\text{in}} = 1$ and $r_{\text{out}} = 25$.

If we were to assume a physical mass scale of $1M_\odot$ and a length scale of 1 au, the central star would have a mass of $1M_\odot$, the circumstellar disc would have a mass of $0.1M_\odot$, or $0.25M_\odot$, and would extend from 1 au to 25 au, and 1 year would equal 2π code units.

2.3 Cooling

Since the aim of this work is to test whether the results obtained by Gammie (2001) using a local model still hold globally, we use the same approach in our global model as used in the local model. We use an adiabatic equation of state, with adiabatic index $\gamma = 5/3$, and allow the disc gas to heat up due to both PdV work and viscous dissipation. Cooling is implemented by adding a simple cooling term to the energy equation. Specifically, for a particle with internal energy per unit mass u_i ,

$$\frac{du_i}{dt} = -\frac{u_i}{t_{cool}} \quad (2)$$

where, as in Gammie (2001), t_{cool} is given by $\beta\Omega^{-1}$ with the value of β varied for each run.

Although the use of the above cooling time is essentially chosen to compare the local model results with results using a global model, it can also be related (at least approximately) to the real physics of an accretion disc. For an optically thick disc in equilibrium, the cooling time is the ratio of the thermal energy per unit area to the radiative losses per unit area. It can be shown (e.g., Pringle 1981) that in such a viscous accretion disc, the cooling time is given by

$$t_{cool} = \frac{4}{9\gamma(\gamma-1)} \frac{1}{\alpha\Omega} \quad (3)$$

where γ is the adiabatic index, Ω is the angular frequency, and α is the Shakura & Sunyaev (1973) viscosity parameter.

3 RESULTS

3.1 $M_{\text{disk}} = 0.1M_*$

We use a global model to consider how cooling times of $t_{cool} = 5\Omega^{-1}$, and $t_{cool} = 3\Omega^{-1}$ affect the gravitational stability of a viscous accretion disc with a mass of $M_{\text{disc}} = 0.1M_*$. Figure 1 shows the disc surface density, Σ , at the beginning and end of the $t_{cool} = 5\Omega^{-1}$ simulation. Since we have not attempted to model the inner boundary condition in any detail, there is rapid accretion and a drop in surface density close to the inner boundary. Apart from particles with radii between 1 and 2 being accreted onto the central star, the surface density profile does not change significantly during the course of the simulation. This also occurs for $t_{cool} = 3\Omega^{-1}$ and a corresponding figure is consequently not shown.

Figure 2 shows the final equatorial density structure of the $t_{cool} = 5\Omega^{-1}$ simulation. The central star (not shown) is located in the middle of the figure and the x and y axes both run from -25 to 25. Figure 3 shows the Toomre Q parameter for the same simulation at the beginning ($t = 0$), approximately a third of the way into the simulation ($t = 876$), and at the end ($t = 2932$) of the simulation. After $t = 2932$ time units, particles at the outer edge of the disk ($r = 25$)

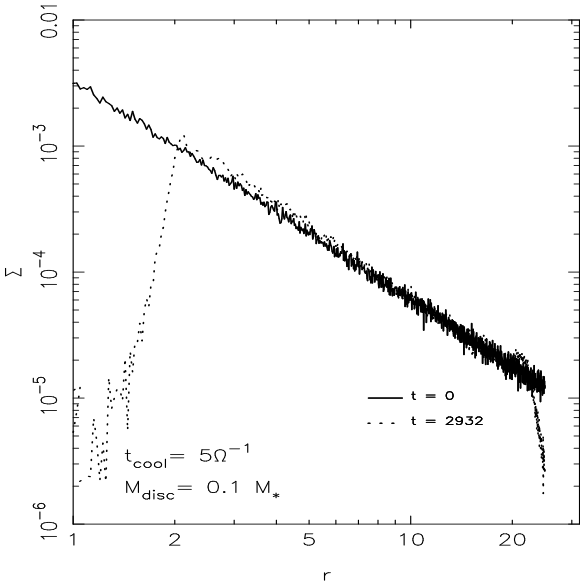


Figure 1. Surface density for $t_{cool} = 5\Omega^{-1}$ and $M_{disc} = 0.1M_*$ at the beginning and end of the simulation. Apart from particles with initial radii between 1 and 2 being accreted onto the central star, the surface density does not change significantly during the simulation.

have completed 3.7 orbits while particles at $r = 1$ have completed 466 orbits. The disc is highly structured and the instability exists at all radii. However, at no point in the disc has the density increased significantly and no fragmentation has taken place. Figure 3 shows that at $t = 2932$ (dashed line) the Toomre Q parameter, which initially had a constant value of 2 (solid line), is close to 1 for radii between 1 and 15. Comparing Q at $t = 876$ and at $t = 2932$ suggests that the cooling may initially reduce Q to below 1, causing the gravitational instability to grow, heating the disc and returning Q to a value of order unity. Figure 3 also shows this region of low Q moving to larger radii with time. This is a consequence of both the cooling time and the dynamical time (the timescale on which heating occurs) both depending directly on radius. The instability therefore starts at the inner radii and by the end of the simulation has reached the edge ($r = 25$) of the disc. The disc has reached a quasi-steady state in which cooling is balanced by heating through viscous dissipation resulting from the growth of the gravitational instability.

Figure 4 shows the final equatorial density structure of the $t_{cool} = 3\Omega^{-1}$ simulation. We were only able to run this simulation for a total of 504 time units and hence Figure 4 shows only the inner 8 radii of the simulation. The central star is again in the middle of the figure. Figure 5 shows the Toomre Q parameter at three different times during the simulation. The initial Q for $t_{cool} = 3\Omega^{-1}$ is the same as for $t_{cool} = 5\Omega^{-1}$ and is therefore not shown in Figure 5. Figure 4 shows that not only is the disc highly structured, the bright dots also indicate that fragmentation is taking place. The fragments that can be seen in Figure 4 are all gravitationally bound. To reach the time shown in Figure 4 it was necessary to convert most of the fragments into point masses (Bate et al. 1995). Figure 5 shows that at $t = 192$ Q is less than 1 for radii between 1 and 5. At later times

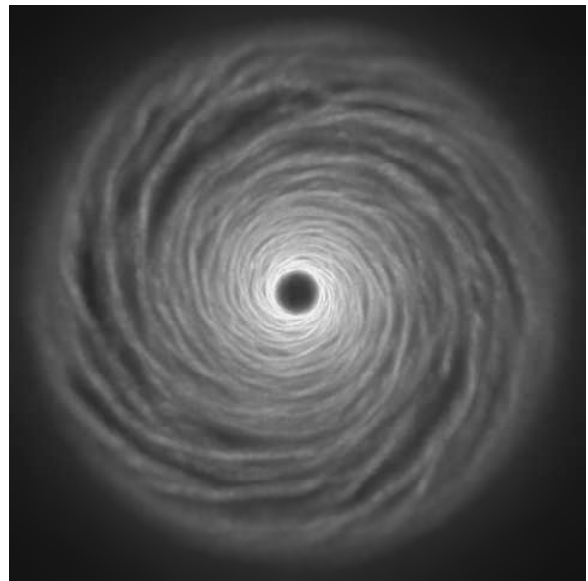


Figure 2. Equatorial density structure for $t_{cool} = 5\Omega^{-1}$ and $M_{disc} = 0.1M_*$. The disc is highly structure with the instability existing at all radii. The density has, however, not increased significantly and the disc is in a quasi-stable state with heating through viscous dissipation balancing cooling.

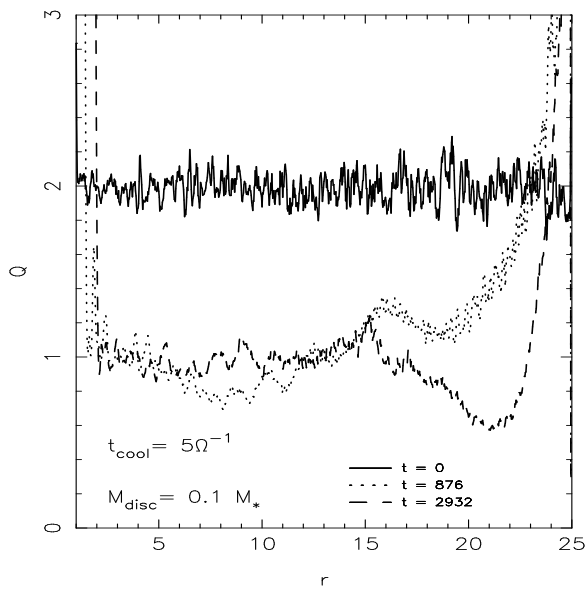


Figure 3. Toomre Q parameter at the beginning ($t = 0$), one third of the way ($t = 876$), and at the end ($t = 2932$) of the $t_{cool} = 5\Omega^{-1}$, $M_{disc} = 0.1M_*$ simulation. At the end of the simulation $Q \sim 1$ at radii between 1 and 15. A low Q region also moves to larger radii with time, indicating the current radius of maximum instability growth.

the minimum Q value moves to larger radii and the value of Q at smaller radii increases to a value of between 1 and 1.5. As in the $t_{cool} = 5\Omega^{-1}$ simulation, the gravitational instability grows from the inner radii and moves to larger radii with time. While Q is below 1, the instability grows rapidly, producing gravitationally bound fragments. These fragments tidally interact with the disc, heating it and causing Q to increase to a value greater than unity. Once $Q > 1$

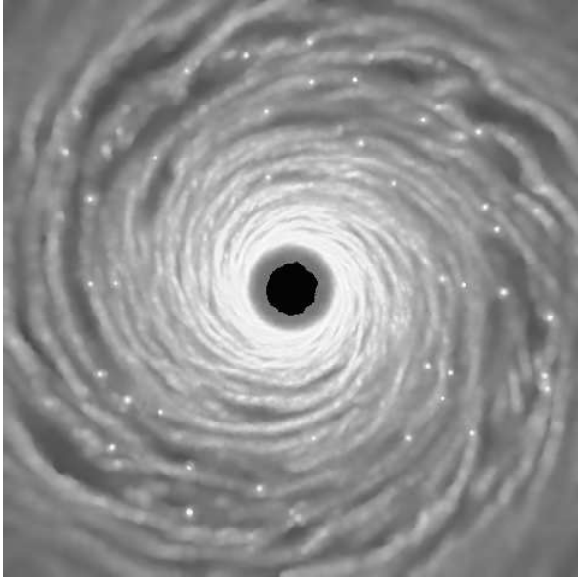


Figure 4. Equatorial density structure for $t_{\text{cool}} = 3\Omega^{-1}$ and $M_{\text{disc}} = 0.1M_*$. The disc is highly unstable and is fragmenting. The fragments are all gravitationally bound.

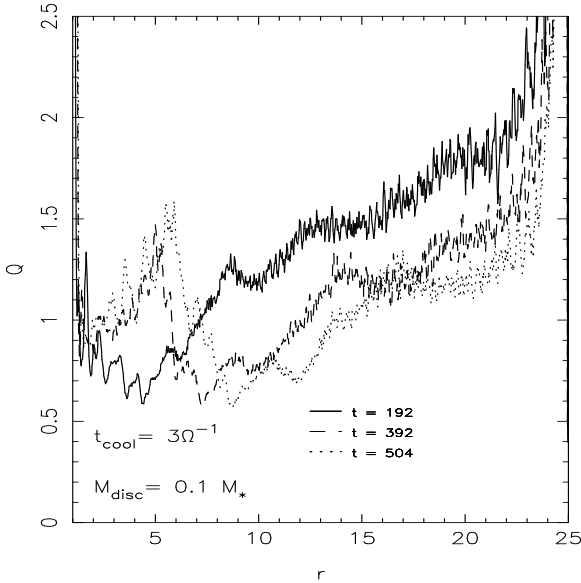


Figure 5. Toomre Q parameter at times of $t = 192$, $t = 362$, and $t = 504$ for $t_{\text{cool}} = 3\Omega^{-1}$ and $M_{\text{disc}} = 0.1M_*$. The value of Q is reduced such that fragmentation of the disc takes place. A region of low Q moves to larger radii with time, indicating the current fragmentation radius.

fragmentation ceases, and the disc, at that radius, becomes gravitationally stable. There is, however, likely to be a significant amount of angular momentum transport driven by tidal interactions between fragments and the gaseous disc (Larson 2002).

Simulations using $t_{\text{cool}} = 10\Omega^{-1}$ and $t_{\text{cool}} = 4\Omega^{-1}$ were also performed. Both simulations were run for more than 2000 time units, almost 4 times longer than the $t_{\text{cool}} = 3\Omega^{-1}$ simulation. The $t_{\text{cool}} = 10\Omega^{-1}$ simulation showed no noticeable structure and the Toomre Q settled down to a value

between 1 and 2. For $t_{\text{cool}} = 4\Omega^{-1}$ the disc structure was similar to that obtained using $t_{\text{cool}} = 5\Omega^{-1}$ except for the presence of a few high density clumps at radii of ~ 10 and greater. By the end of the simulation ($t = 2136$) one of the clumps, at a radius of 9.5, had satisfied the condition for point mass creation, i.e. it was gravitationally bound. This would suggest that, globally, fragmentation may occur at slightly greater cooling time than expected using a local model (Gammie 2001). However, unlike the $t_{\text{cool}} = 3\Omega^{-1}$ simulation, the $t_{\text{cool}} = 4\Omega^{-1}$ simulation did not fragment at all radii, with the inner ~ 10 radii of the disc remaining in a quasi-stable state.

3.2 $M_{\text{disc}} = 0.25M_*$

A simulation using a heavier disc ($M_{\text{disc}} = 0.25M_*$) was also performed. Although most T Tauri discs have masses significantly less than this (Beckwith et al. 1990), there are a few with comparable masses. Such a simulation may also be appropriate for an earlier stage of the star formation process when the discs are expected to be heavier. We considered cooling times of $t_{\text{cool}} = 10\Omega^{-1}$ and $t_{\text{cool}} = 5\Omega^{-1}$. The $t_{\text{cool}} = 10\Omega^{-1}$ simulation was run for 1024 time units, at the end of which, as for $M_{\text{disc}} = 0.1M_*$, the disc showed minimal structure and there was no sign of any density enhancement or fragmentation.

The $t_{\text{cool}} = 5\Omega^{-1}$ simulation was run for 684 time units and the final equatorial density structure is shown in Figure 6. The disc is highly structured and the spirals, consistent with the increased disc mass (Nelson et al. 1998), are somewhat less filamentary than for the $M_{\text{disc}} = 0.1M_*$ simulation with the same cooling time. Unlike the equivalent $M_{\text{disc}} = 0.1M_*$ simulation (see Figure 2) there are, however, a number of high density clumps present in the disc. The routine for converting these clumps into point masses checks the nearest ~ 50 SPH particles to determine if they are gravitationally bound (see Bate et al. 1995). Using this technique, the high density regions in Figure 6 were found to be gravitationally unbound and could not be converted into point masses. The simulation was eventually stopped at $t = 684$ when the maximum density had increased to a value 10^7 times greater than the initial maximum density. Restricting the determination of the boundness of the clump to only the nearest ~ 50 SPH particles is somewhat arbitrary. By including the nearest ~ 250 SPH particles, rather than only the nearest ~ 50 , the densest clump was found to be just gravitationally bound, i.e. the gravitational potential energy was almost exactly twice the thermal energy. This would imply that in more massive discs, global effects could act to make the disc more unstable, allowing gravitationally bound fragments to grow for cooling times greater than that obtained using a local model. This may have implications both for the formation of planets, or binary companions (Adams, Ruden & Shu 1989), reasonably early in the star formation process.

3.3 Cooling time and effective viscosity

By using a radially dependent cooling time in our simulations, Equation (3) implies that the discs should settle into a state in which the effective viscous α (Shakura & Sunyaev

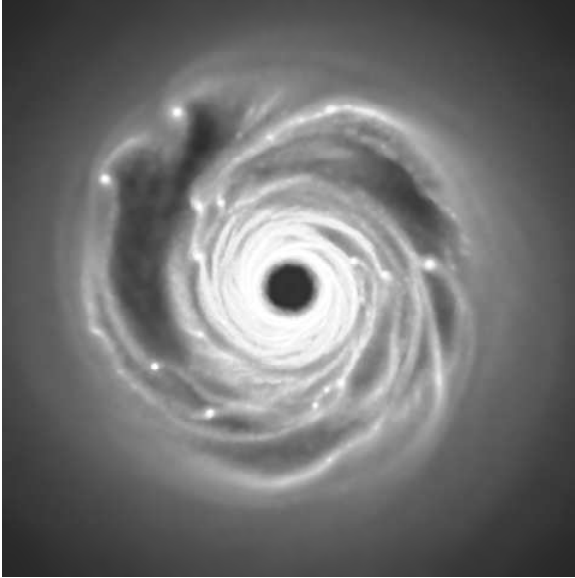


Figure 6. Equatorial density structure for $t_{\text{cool}} = 5\Omega^{-1}$ and for a disc mass $M_{\text{disc}} = 0.25M_*$. There are signs of fragmentation with the most massive fragment being gravitationally bound.

1973) depends inversely on this cooling time. Since none of our simulations were run to a steady state, which would take several viscous times to achieve, it is not straightforward to determine whether the local scaling of α with t_{cool} is obeyed. This is further complicated in the $t_{\text{cool}} = 3\Omega^{-1}$, $M_{\text{disc}} = 0.1M_*$ simulation since the collapsed mass fraction increases throughout the run. We are, however, able to compare the $t_{\text{cool}} = 5\Omega^{-1}$, $M_{\text{disc}} = 0.1M_*$ simulation with the $t_{\text{cool}} = 10\Omega^{-1}$, $M_{\text{disc}} = 0.1M_*$ simulation. Figure 7 shows the magnitude of the mass transfer rate through a radius $r = 15$, plotted against time in code units, for $t_{\text{cool}} = 5\Omega^{-1}$ (solid line) and $t_{\text{cool}} = 10\Omega^{-1}$ (dashed line) and a disc mass, in both cases, of $M_{\text{disc}} = 0.1M_*$. Figure 7 only considers the mass transfer rate once the instability has almost saturated at the radius considered. Since neither simulation has reached a steady state and since both discs are self-gravitating, the mass transfer rate can be negative or positive. Figure 7 is consequently a 60 time unit running average of the magnitude of the mass transfer rate and shows that the mass transfer rate for $t_{\text{cool}} = 5\Omega^{-1}$ is, as expected, higher than that for $t_{\text{cool}} = 10\Omega^{-1}$. By the end of simulation the mass transfer rates are both reasonably constant and differ by a factor of between 2 and 3. Although this difference is consistent with that expected from Equation (3), the complications in trying to accurately determine the relationship between α and t_{cool} in these global simulations leads us to simply conclude that, as expected, the effective viscosity does indeed increase with decreasing cooling time.

4 CONCLUSION

Using a local model, Gammie (2001) has shown that for cooling times $t_{\text{cool}} \leq 3\Omega^{-1}$ a disc will fragment into one or more gravitationally bound objects, while for longer cooling times the disc will settle into a quasi-stable state with heating through viscous dissipation balancing cooling. We have

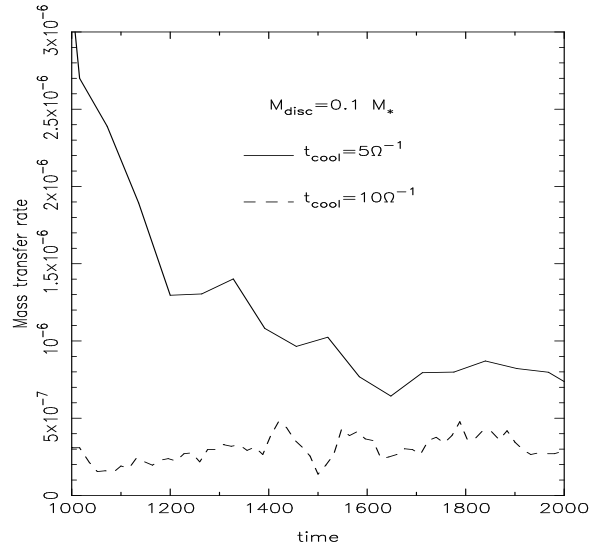


Figure 7. A running average of the magnitude of the mass transfer rate for $t_{\text{cool}} = 5\Omega^{-1}$ and $t_{\text{cool}} = 10\Omega^{-1}$ and for a disc mass $M_{\text{disc}} = 0.1M_*$.

performed three-dimensional disc calculations using SPH to test if the above still holds globally. We use the same cooling function as used by Gammie (2001) which, although fairly simplistic, can also be justified physically (Pringle 1981).

For a disc mass of $M_{\text{disc}} = 0.1M_*$ and for cooling times of $t_{\text{cool}} = 5\Omega^{-1}$ and $t_{\text{cool}} = 10\Omega^{-1}$ we find that the disc settles into a quasi-stable state. At the end of the $t_{\text{cool}} = 5\Omega^{-1}$ run, the Toomre Q parameter is of order unity between radii of 1 and 15 and the disc is highly structured. The density is, however, not significantly greater than the initial density and no fragmentation has occurred. A comparison between the $t_{\text{cool}} = 5\Omega^{-1}$ and the $t_{\text{cool}} = 10\Omega^{-1}$ simulations also shows that once the instability has saturated at a given radius, the magnitude of the mass transfer rate was greatest for the smaller cooling time. Although we were unable to quantify the relationship between the cooling time and the viscous α (Shakura & Sunyaev 1973), this result shows that, as expected, the effective viscosity does indeed increase with decreasing cooling time.

For $t_{\text{cool}} = 3\Omega^{-1}$ the disc rapidly becomes unstable and produces numerous gravitationally bound fragments. The growth of these fragments starts near the inner boundary of the disc and had we been able to continue with the simulation, it seems likely that fragmentation would have continued throughout the disc. A $t_{\text{cool}} = 4\Omega^{-1}$ simulation also produced gravitationally bound fragments but these were located at radii of ~ 10 or greater. The inner radii of the disc remained in a quasi-steady state.

A simulation using a heavier disc ($M_{\text{disc}} = 0.25M_*$) was found to fragment for cooling times of $t_{\text{cool}} = 5\Omega^{-1}$, suggesting that as the disc mass increases, global effects may act to make the disc more unstable. A cooling time of $t_{\text{cool}} = 10\Omega^{-1}$, however, showed no signs of fragmentation and hence the fragmentation boundary, even for the heavier disc, is still within a factor of ~ 2 of that obtained using a local model (Gammie 2001). For T Tauri discs, which generally have masses $M_{\text{disc}} < 0.1M_*$ (Beckwith et al. 1990), the fragmentation boundary is therefore likely to be close to

that determined using the local model. Earlier in the star formation process, when the discs are expected to be more massive, fragmentation may occur for cooling times somewhat longer than that predicted by the local model results (Gammie 2001).

For quiescent T Tauri discs, α is conventionally estimated to be of the order of 10^{-2} or smaller (Hartmann et al. 1998; Bell & Lin 1994). The simple estimates quoted earlier would suggest that such discs are comfortably stable. Boss (2001), however, has shown using an approximate treatment of the disc heating and cooling that there may be periods when the cooling time is comparable to the orbital period. Our results suggest that if the disc is fairly massive, such short cooling times open a window of opportunity for the formation of substellar objects, probably in the form of a multiple system (Armitage & Hansen 1999). Not only does this have implications for planet formation in protoplanetary discs, it also has implications for angular momentum transport. The presence of a number of massive clumps within a protoplanetary disc is likely to significantly enhance the transport of angular momentum through tidal interactions (Larson 2002). Similar considerations apply to AGN discs. Numerous theoretical studies (e.g. Clarke 1988; Kumar 1999; Hure 2000; Menou & Quataert 2001) show that AGN discs invariably become self-gravitating at radii of ~ 0.1 pc. Fragmentation would lead to the formation of stars (Collin & Zahn 1999), and truncation of the inner accretion disc (Goodman 2002). Instability of gaseous discs at much larger radii of $10 - 1000$ pc may also occur (Shlosman & Begelman 1989). Fragmentation of these larger scale discs would yield a flattened stellar system, while rapid angular momentum transport could play a role in replenishing the inner galactic reservoir (Shlosman & Begelman 1989).

ACKNOWLEDGMENTS

The simulations reported in this paper made use of the UK Astrophysical Fluids Facility (UKAFF). WKMR acknowledges support from a PPARC Standard Grant.

REFERENCES

Adams F.C., Ruden S.P. & Shu F.H., 1989, *ApJ*, 347, 959.
 Armitage P.J. & Hansen B.M.S., 1999, *Nature*, 399, 633.
 Balbus S.A., Papaloizou J.C.B., 1999, *ApJ*, 521, 650.
 Bate M.R., Bonnell I.A., Price N.M., 1995, *MNRAS*, 277, 362.
 Beckwith S.V.W., Sargent A.I., Chini R.S., Guesten R., 1990, *AJ*, 99, 924.
 Bell K.R. & Lin D.N.C., 1994, *ApJ*, 427, 987.
 Benz W., 1990, in Buchler J.R., ed, *The Numerical Modeling of Nonlinear Stellar Pulsations*, Kluwer, Dordrecht, p. 269.
 Boss A.P., 1998, *Nature*, 393, 141.
 Boss A.P., 2000, *ApJ*, 536, L101.
 Boss A.P., 2001, *ApJ*, 563, 367.
 Clarke C.J., 1988, *MNRAS*, 235, 881.
 Collin S. & Zahn J.-P., 1999, *A&A*, 344, 433.
 Gammie C.F., 2001, *ApJ*, 553, 174.
 Goldreich P., Lynden-Bell D., 1965, *MNRAS*, 130, 125.
 Goodman, J., 2002, *MNRAS*, submitted.
 Hartmann L., Calvet N., Gullbring E. & D'Alessio P., 1998, *ApJ*, 495, 385.
 Huré J.-M., 2000, *A&A*, 358, 378.
 Kim W-T, Ostriker, E.C., 2002, *ApJ*, 570, 132.
 Kuiper G.P., 1951, in Hynek J.A., ed, *Proceedings of a topical symposium, commemorating the 50th anniversary of the Yerkes Observatory and half a century of progress in astrophysics*, McGraw-Hill, New York, p. 357.
 Kumar P., 1999, *ApJ*, 519, 599.
 Larson R.B., 2002, *MNRAS*, 332, 155.
 Lissauer J.J., 1993, *ARA&A*, 31, 129.
 Marcy G.W., Butler R.P., 2000, *PASP*, 112, 137.
 Mayor M., Queloz D., 1995, *Nature*, 378, 355.
 Menou K. & Quataert E., 2001, *ApJ*, 552, 204.
 Monaghan J.J., 1992, *ARA&A*, 30, 543.
 Navarro J.F., White S.D.M., 1993, *MNRAS*, 265, 271.
 Nelson A.F., Benz W., Adams F.C. & Arnett D., 1998, *ApJ*, 502, 342.
 Pickett B.K., Cassen P., Durisen R.H. & Link R., 1998, *ApJ*, 504, 468.
 Pickett B.K., Durisen R.H., Cassen P. & Mejia A.C., 2000, *ApJ*, 540, L95.
 Pringle J.E., 1981, *ARA&A*, 19, 137.
 Shakura N.I., Sunyaev R.A., 1973, *A&A*, 24, 337.
 Shlosman I., Begelman M., 1989, *ApJ*, 341, 685.
 Toomre A., 1964, *ApJ*, 139, 1217.
 Yorke H.W., Bodenheimer P., 1999, *ApJ*, 525, 330.